Fermi National Accelerator Laboratory

FERMILAB-Pub-94/384

Fluctuations of Muon Energy Loss and Simulation of Ionization Cooling

A. Van Ginneken

Fermi National Accelerator Laboratory
P.O. Box 500, Batavia, Illinois 60510

January 1995

Nuclear Instruments & Methods

Operated by Universities Research Association Inc. under Contract No. DE-AC02-76CHO3000 with the United States Department of Energy

Disclaimer

Fluctuations of Muon Energy Loss and Simulation of Ionization Cooling

A. Van Ginneken
Fermi National Accelerator Laboratory*
P. O. Box 500, Batavia, IL 60510

November 1994

Abstract

A Monte Carlo program to simulate muon ionization cooling is outlined. A Vavilov-type distribution to represent *restricted* ionization energy losses is derived. Above the restriction threshold μe scattering is treated event-by-event. Likewise μ-nucleus elastic scattering is simulated by a Gaussian below some angular threshold and treated individually above it. Other processes included are: incoherent μp scattering with nuclear protons, bremsstrahlung, pair production, and deep inelastic nuclear scattering. A small sample of results obtained with the code is included.

1 Introduction

Ionization cooling of muons is often mentioned in connection with muon storage rings, which—of late—have enjoyed considerable interest as an alternative to high energy ee linear colliders. For a review of the subject and further references, see [1, 2]. Briefly, the muon beam is recirculated through a cooling target while an RF field makes up for average energy lost in the target. This acts on both transverse and longitudinal phase space. Muons lose transverse as well as longitudinal momentum in the target while only

*Work supported by the U.S. Department of Energy under contract No. DE-AC02-76CHO3000.

the latter is restored by the RF thus resulting in a net transverse phase space reduction. Other processes which occur in the target—principally multiple Coulomb scattering—counteract the cooling and must be included in the analysis. Longitudinally, cooling is said to take place when the muon energy is in the 'relativistic rise' regime of the dE/dx *vs* E curve since there the more energetic muons suffer a larger energy loss. But this is true *only in the mean*. Typically, the spread in energy loss incurred traversing a target far exceeds any cooling achievable from the difference in dE/dx. In fact, most of the relativistic rise in dE/dx is due to the concomitant increase in the maximum energy which can be imparted to an atomic e^-. Thus the extra energy loss is due to relatively large energy transfers which may well cause net heating or even removal of the muon from the beam. This depends on muon energy as well as on initial and (desired) final longitudinal phase space. More promising is the proposal to place a wedge-shaped cooling target in a region of high momentum dispersion so that the more energetic muons traverse a thicker target and thus lose more energy. Like in the transverse case, longitudinal heating due to fluctuations in ionization energy loss and other processes occurs in the target and should be incorporated in the simulation.

Analyses of cooling, such as ref. [2], use a differential equation to describe the *average* change in emittance—separately for transverse and longitudinal phase space. Clearly some detail about the *distribution* in phase space is desirable. Correlations between transverse and longitudinal degrees of freedom are also expected to be present. Moreover, beam loss in a cooling ring is a *first passsage* problem, i.e., a muon experiencing a large enough energy loss or angular deflection leaves permanently its RF bucket or the admittance of the ring—without prospect of rejoining the beam by means of some subsequent fluctuation. These effects are disregarded in the differential equation approach. In addition there are other processes to be considered: incoherent nuclear scattering, bremsstrahlung, pair production, and nuclear interaction of muons—all of which increase in importance with energy. Typically, these relatively rare processes cause large energy losses and are therefore best treated as individual events. These are the key concerns addressed in this note and which form the basis of a Monte Carlo simulation program (SIMUCOOL).

In sec. 2 the treatment of ionization losses in the simulation is described in some detail. This may be of interest for applications other than ionization cooling. Coulomb scattering is the subject of sec. 3. The remaining processes considered are relegated to sec. 4. Some results of a rather general nature on muon cooling are presented in sec. 5 along with a small sample of results

from the program but without launching into a systematic investigation of the subject. Concluding remarks are in sec. 6.

2 Ionization Loss

This section arrives at the formulae necessary to treat ionization losses in a Monte Carlo simulation. Some modifications to commonly used energy loss distributions are described which (1) make them specific to muons by use of Bhabha's scattering law for spin *(J)=1/2* particles on electrons and (2) allow introduction of a ***restriction threshold*** of the energy loss in a single collision leaving larger losses to be treated as individual events and thus incorporate energy-angle correlations into the simulation. In connection with this last point it should be remembered that Coulomb scattering off nuclei is a larger source of angular dispersion than that off atomic electrons and the nuclear part is essentially uncorrelated with energy loss. Nonetheless, an accurate description of the phase space should include correlations present in the μe part.

2.1 Vavilov's Distibution for J=1/2

The distribution of ionization energy loss of a high energy particle traversing a target was first derived by Landau [3]. Specifically, Landau assumes that the probability of an energy loss, ϵ, in a single collision, follows an ϵ^{-2} law and that total energy loss is small compared to ϵ_{max} (or that $\epsilon_{max} \to \infty$). Vavilov [4] refined Landau's procedure by including the (kinematically allowed) maximum energy loss in the derivation and adopting a more accurate $\epsilon^{-2}(1 - \beta^2\epsilon/\epsilon_{max})$ energy loss law, with β—as usual—the velocity in units of c. One price to pay for these refinements is that, whereas the Landau distribution can be represented by a single universal curve, Vavilov's depends on two parameters: β and $\kappa = 0.300465 x m_e Z/(\beta^2 A \epsilon_{max})$ where the latter is primarily a measure of target thickness, x (in $g{\cdot}cm^{-2}$). Tables of Vavilov's distribution are presented in [5]. Other modifications to the formulae of Landau and Vavilov are necessary for very thin targets [6] but these can presumably be neglected in the present context.

The energy loss law assumed by Vavilov is correct for *J=0* particles. For *J=1/2* particles—such as muons—it becomes [7]

$$P(\epsilon) \propto \epsilon^{-2}\left[1 - \beta^2\frac{\epsilon}{\epsilon_{max}} + \frac{1}{2}\left(\frac{\epsilon}{E_0}\right)^2\right] \qquad (1)$$

where E_0 is the total energy of the incident particle. It is a simple matter to repeat Vavilov's procedure with Bhabha's formula which yields (in the notation of ref. [4])

$$f(x,\Delta) = \frac{1}{\pi\epsilon_{max}} e^{\kappa(1+\beta^2 C - R^2/2)} \int_0^\infty e^{\kappa F_1} cos\,(y\Lambda_1 + \kappa F_2)\,dy \qquad (2)$$

where Δ means total energy loss in the sample and

$$F_1 = \beta^2\,[\ln y - Ci(y)] - \cos y - ySi(y) + \frac{R^2}{2}\frac{\sin y}{y} \qquad (3)$$

$$\Lambda_1 = \frac{\Delta - \overline{\Delta}}{\epsilon_{max}} - \kappa\left(1 + \beta^2 - C - \frac{R^2}{4}\right) \qquad (4)$$

$$F_2 = y\,[\ln y - Ci(y)] + \sin y + \beta^2 Si(y) - \frac{R^2}{2}\frac{1-\cos y}{y}. \qquad (5)$$

Here $R = \epsilon_{max}/E_0$ while Si and Ci are the sine and cosine integrals and C is Euler's constant. Setting $R=0$ corresponds to Vavilov's expression and F_1, F_2, Λ_1 revert to f_1, f_2, λ_1 of Vavilov's paper. Λ_1 is related to Landau's λ by

$$\Lambda_1 = \kappa\left(\lambda + \frac{R^2}{4} + \ln\kappa\right). \qquad (6)$$

Differences between $J=0$ and $1/2$ are not very large. Fig. 1 compares (in the manner of ref. [4]) the quantity $\phi = \kappa\epsilon_{max} f$ plotted as a function of Landau's λ for β=1 (which implies R=1) and for κ=0.1, 1, and 10 [8]. As might be expected the $J=1/2$ distribution is slightly broadened vis-a-vis $J=0$.

2.2 Distribution for Restricted Loss

Perhaps more relevant to the present application than specialization to $J=1/2$ is the introduction into eq. 2 of an—essentially arbitrary—energy loss limit in a single collison, ϵ_c. Losses below ϵ_c can then be included on a statistical basis via a Vavilov-type distribution while those above it are treated individually.

Again Vavilov's procedure (for $J=1/2$) is easily applied to the restricted ionization loss case. All that is necessary is to replace ϵ_{max} everywhere by ϵ_c except in Bhabha's scattering law which is, of course, unaffected by introducing an arbitrary ϵ_c. The result is

$$f(x,\Delta) = \frac{1}{\pi\epsilon_c} e^{\kappa(1+\beta^2 SC - R_c^2/2)} \int_0^\infty e^{\kappa\mathcal{F}_1} cos\,(y\mathcal{L}_1 + \kappa\mathcal{F}_2)\,dy \qquad (7)$$

where

$$\mathcal{F}_1 = \beta^2 S\left[\ln y - Ci(y)\right] - \cos y - ySi(y) + \frac{R_c^2}{2}\frac{\sin y}{y} \tag{8}$$

$$\mathcal{L}_1 = \frac{\Delta - \overline{\Delta_c}}{\epsilon_c} - \kappa\left(1 + \beta^2 S - C - \frac{R_c^2}{4}\right) \tag{9}$$

$$\mathcal{F}_2 = y\left[\ln y - Ci(y)\right] + \sin y + \beta^2 SSi(y) - \frac{R_c^2}{2}\frac{1-\cos y}{y}. \tag{10}$$

Now $R_c = \epsilon_c/E_0$, $\overline{\Delta_c}$ is the average restricted energy loss (below ϵ_c as in, e.g., ref. [9]) and $S = \epsilon_c/\epsilon_{max}$. Setting $\epsilon_c = \epsilon_{max}$ leads back to eq. 2. Setting $R_c = 0$ yields Vavilov's ($J = 0$) distribution for restricted losses.

2.3 Implementation

It is evident that random selection of an energy loss in a Monte Carlo simulation is not feasible by analytical means, i.e., by inverting eq. 7. Even an accurate direct numerical calculation of eq. 7 requires significant computation time. However the present application lends itself to some simplifications. First, all muons in any given cooling scenario will have nearly the same β. As may be verified, the Vavilov distribution is not very sensitive to small changes in β. Therefore β may be considered constant in any given simulation and fixed at, e.g., β corresponding to the nominal muon energy. A second simplification is use of a fixed steplength for muon transport—which fixes κ for a given material. If, as anticipitated in a typical cooling scenario, a single target material is used then a single (tabulated) distribution suffices to treat the problem of ionization loss fluctuations. Use of a fixed steplength entails some corrections for edge effects. Needless to say, one can always resort to multiple tables and interpolation between them for increased accuracy.

Integration of eq. 7 requires some care. The cosine in the integrand causes large cancellations after which a small positive number remains. A sure-footed way to proceed is to first locate the zeroes of the integrand (cosine) using Newton's method and then to perform Romberg integration between the zeroes as intermediate limits until the contribution from a complete cycle of the cosine argument falls below some small fraction of the cumulative total. $\mathcal{L}_1$ of eq. 9 is used as the variable of the distribution which easily converts into an energy loss.

The choice of ϵ_c is left free in the Monte Carlo implementation. A smaller ϵ_c results in higher accuracy at the expense of longer computation times.

Selection of ϵ larger than ϵ_c is made directly from Bhabha's formula by choosing from an ϵ^{-2} distribution between ϵ_c and ϵ_{max} and taking account of the part of eq. 1 in square brackets by means of 'rejection'. Because μe scattering is essentially a two-body process energy loss correlates uniquely with angle acquired, viz., $\theta = \sqrt{2m_e\epsilon}/p_\mu$ in the small angle approximation.

3 Coulomb Scattering

Coulomb scattering of muons can proceed coherently—off the entire nucleus which remains in its ground state—or incoherently, where the muon scatters off an individual nuclear proton which gets ejected or promoted to an unoccupied state. Similar in spirit to the treatment of ionization losses, below some cut-off angle coherent scattering is treated as multiple scattering while for larger angles it is simulated as complete individual events.

3.1 Multiple Coulomb Scattering

According to [10] the Gaussian approximation for projected angles in multiple scattering holds quite well for angles below about 2σ—independent of target thickness. For larger angles the Gaussian becomes quickly submerged in the single scattering tail which suggests that 2σ is a reasonable choice for θ_c, the (spatial) cut-off angle, i.e., $\theta_c = 2 \cdot 0.0192\sqrt{\ell/X_0}$, where ℓ is a (fixed) step length, and X_0 is the radiation length of the material. For spatial angles (θ_s) the Gaussian corresponds to an exponential distribution in θ_s^2.

The introduction of θ_c means a lower σ compared with the usually cited overall *rms* scattering angle. From [11] one obtains

$$\langle\theta_s^2\rangle = 4\pi N_{Av}\rho\ell\alpha^2(Z^2/A)\left[\ln\left(\frac{\theta_c^2}{\theta_1^2}+1\right)-1\right] \tag{11}$$

where N_{Av} is Avogadro's number, ρ the density of the material, α the fine-structure constant, and $\theta_1 = \alpha m_e Z^{1/3}$ is an effective lower angular limit based on screening of the nuclear charge by atomic electrons.

3.2 Coherent

Above θ_c the Rutherford scattering formula is used directly. Spin corrections introduce a weak dependence on nuclear species but are of even lesser importance here than for energy loss off atomic e^- and can be neglected. However,

Rutherford's formula must be modified by a form factor to suppress large momentum transfers (which may break apart the nucleus and destroy the coherence). A simple form factor [13] is applied: $F_N = (1 + t/d)^2$ where $d = 0.164A^{-2/3}\ \ GeV^2$ and t is the absolute value of the 4-momentum transfer. Monte Carlo implementation of this process begins by choosing a random number of events from a Poisson distribution based on the expected number in a single step. For each event—if any—an angle ($> \theta_c$) is selected from Rutherford's formula while the form factor is included by rejection. A (small) momentum loss resulting from each encounter is applied to the muon.

3.3 Incoherent

Muons can also interact (incoherently) with individual protons inside the nucleus causing the struck proton to be either ejected or promoted to an (unoccupied) higher energy level. The model is somewhat easier to state in terms of momentum transfer rather than angle. In full, the basic μp scattering law is given by the Rosenbluth formula [12]. However, since the nuclear model used here is rather crude it makes more sense to again rely on Rutherford's formula for (Z times) μp

$$d\sigma/dt = 4\pi Z(\alpha/t)^2 \tag{12}$$

modified by a proton form factor which damps high momentum transfers that may be accompanied by particle production (the latter is treated as a separate contribution, see sec. 4). From ref. [13]:

$$F_p = \frac{1 + 7.78\tau}{(1+\tau)(1+\tau/0.71)^4} \tag{13}$$

with $\tau = t/4m_p^2$. The nucleus is approximated by a simple Fermi gas of the constituent nucleons and a struck proton must acquire a final momentum larger than the Fermi momentum for the collision to be allowed. On kinematical grounds the energy transfer to the proton is required to be in excess of $\mathcal{E}_{gap}$ which corresponds to the first excited level of the target nucleus. This mimimum transfer also assigns a convenient upper limit of $4\pi Z\alpha^2/t_{min}$ to the total cross section, where t_{min} is approximated by $2m_p\mathcal{E}_{gap}$, its value for a proton at rest. Cuts on final momentum and effects of the proton form factor are simulated by rejection. Experimental values of $\mathcal{E}_{gap}$ are provided for a few commonly used target nuclei with a 1 MeV default value elsewhere.

The total cross section is small enough that one can safely neglect multiple μp scatterings in a single nuclear encounter.

When an event occurs on the basis of the above cross section, the algorithm proceeds by (i) selecting a Fermi momentum for the proton partner—but with only $|p_z|$ determined at this point. The sign of p_z is randomly assigned according to the flux factor $(E - p_z)/2E$ which favors 'head-on' over 'rear-end' collisions [14]. (ii) A value for $t \geq t_{min}$ is then selected and tested by comparing a uniform random number *vs* the proton form factor. If larger, the entire event is rejected. If smaller, (iii) final momenta are determined in the μp center of mass and transformed back to the lab. Finally, (iv) it is determined if the struck proton emerges above the Fermi sea. If not, the event is scrapped.

While refinements are obviously possible, see e.g. [15], such a model appears to describe quasi-elastic e^-–nucleus collisions quite well even for light nuclei [14].

4 Other Processes

Three more processes are included which are important mainly at higher energies: bremsstrahlung, direct pair production, and deep inelastic nuclear interactions by the muons. All are fairly 'hard' processes in which a muon typically loses considerable energy making them potentially important for the present application. The procedures followed for each process are those described in some detail in [16]. Briefly, energy loss is determined randomly from an empirical function which represents a fit to results of more complicated *ab initio* calculations. For a given energy loss the *rms* angle, $\langle\theta^2\rangle^{1/2}$, is found from another empirical formula which also approximates more accurate calculations. A random angle is then selected from a *Gaussian* with zero mean and $\sigma = \langle\theta^2\rangle^{1/2}$. This scheme is perhaps easier to justify for muon shielding calculations for which it is intended but it is adopted here as well. The angles incurred tend to be small compared with Coulomb scattering and—at least to first order—some correlation between angle and energy loss is kept so that no large error is expected as a result of adopting this procedure.

5 Results

This section aims to provide a few results of the SIMUCOOL model, mostly by way of illustration. There are too many parameters to attempt any type of systematic coverage here: specification of the initial muon beam in 6-D phase space, lattice of the cooling ring (or linac), thickness (or description of more complicated geometry—such as wedges) and composition of the target, its location(s) in the cooling ring along with any electric or magnetic fields which may be present at the target location. One must also specify how and where the restoring momentum is delivered, what are the criteria for removal from the beam as well as the number of turns over which to cool. In any given application the choices are likely to be considerably narrowed since many parameters will be specified or at least delimited by other considerations.

One set of results which is generally useful is the expected number of events per unit length of target material in which an energy loss or angular threshold is *exceeded in a single collision.* This puts a lower limit on the number of particles acquiring such an energy loss or angular divergence since others may do so as a result of multiple encounters. Fig. 2 shows the number of events with $\Delta E/E$ above 0.03, 0.1, and 0.3 for a lithium target for each contributing mechanism as a function of muon energy. Fig. 3 is the corresponding plots for tungsten. Fig. 4 displays the *total* number of such events for four target materials. The double hump for $\Delta E/E > 0.3$ reflects peaks in the energy dependence of deep inelastic nuclear scattering and large angle scattering off atomic e^-, whereas the latter dominates completely for $\Delta E/E < 0.03$. In a similar vein, fig. 5 shows total number of events per cm of target with $\Delta\theta$ above 0.01 and 0.05 radians as a function of energy for four materials. Bremsstrahlung, pair production, and deep inelastic scattering are omitted from consideration for these plots. These are not expected to make a significant contribution. As mentioned in sec. 4 these are treated in the simulation using the Gaussian approximation which would be unsuitable for inclusion in fig. 5, i.e., on a single event basis.

By way of example, some results are presented of a simulation on a sample of 2500 muons of 1 GeV recirculating through a 1 cm thick beryllium target. The initial phase space is taken to be biGaussian both in x,x' and in y,y' with (nominal) transverse emittances $\epsilon_x = \epsilon_y = 10^{-4}$ and with $\beta_x = \beta_y = 1$ cm. Particles with x,x' (y,y') above 3σ are excluded (which reduces initial emittances by about 0.15). The longitudinal emittance is represented by a *uniformly* populated ellipse with axes $\Delta p/p = \pm 0.1$ and $\Delta\phi = \pm 0.35$ rad. Before each traversal of the target the phase space distribu-

tions are rotated (at some rate out of tune with the rotation around the ring). After each traversal the average dE/dx for collision losses corresponding to the nominal muon energy is restored to the muon along the beam direction. Muons which acquire an emittance in excess of *twice* the initial one (either longitudinally or in one of the transverse planes) are dropped from the simulation. Fig. 6 shows (x,y combined) transverse phase space progression with number of traversals. Cooling is clearly observed. For comparison, using Neuffer's formula [17], the equilibrium emittance is $1.67 \cdot 10^{-5}$—or 0.196 on a relative basis—indicating good agreement for transverse phase space. Fig. 7 is the corresponding result for longitudinal space where some 'heating' is equally obvious which strongly suggests that most of the lost muons exit longitudinally.

Fig. 8 presents the Vavilov ($J=1/2$) distribution for 0.5 and 0.55 GeV/c muons traversing a 1 cm beryllium target. The 'knee' around ϵ_{max} is quite noticeable and is peculiar to the $J=1/2$ type. Also in fig. 8 is $\int_0^\Delta \epsilon(f_{0.55} - f_{0.5})\, d\epsilon$ as a measure of how the (cumulative) difference in energy loss is distributed. As indicated, the median occurs close to $\Delta = 0.014$ GeV—well outside the peak. Therefore most of the difference in $\langle\Delta\rangle$ (which amounts to only 33 KeV) is due to relatively rare events while some heating is expected with each traversal. As an estimate of the latter consider the case of two muons (or beams) of 0.5 and 0.55 GeV/c repeatedly traversing a 1 cm beryllium target with energy restoration. Ignoring all processes other than energy loss off atomic e^-, this is equivalent to increasing target thickness while shifting the ordinate (Δ) by the appropriate average energy loss. Fig. 9 shows the distributions after 5, 10, and 25 turns for mono-energetic beams of 0.5 and 0.55 GeV/c. These must yet be folded by the initial momentum distribution of the beam as done in a Monte Carlo simulation. Results of the latter also benefit from including other significant processes as well as the first passage effect which becomes important when the energy spread approaches that which can be accommodated by the RF.

6 Concluding Remarks

When the simulation is run neglecting all processes except multiple Coulomb scattering and with constant energy loss replenished along the beam direction, results for transverse emittance essentially confirm the conclusions of ref. [2]: the difference between initial and equilibrium emittance decays exponentially with number of traversals and with decay constant proportional

to the fractional energy loss per traversal.

Matters become more complicated when other processes are included and limits are imposed on both longitudinal and transverse phase space. In transverse phase space the picture remains by and large correct but net longitudinal heating results in the example. Note that in fig. 7 the stated longitudinal emittance growth is considerably biased downward by excluding muons with emittances larger than twice the initial one. However, simply removing such exclusionary limits appears even less useful because it is unrealistic to expect particles at a large emittance to remain with the beam and also because a few 'outliers' can easily distort statistics such as the average emittance—particularly in a relatively small sample. A downward bias is expected to be present in the transverse case as well since some particles may be lost by exiting the transverse phase space. However, judging from fig. 6 this bias appears to be minimal. These results thus tend to confirm the reservations expressed in the introduction about longitudinal cooling via the relativistic dE/dx rise and it appears that one must resort to wedges or more complicated geometries to do the job. In general, the relation between muon energy and cooling efficiency appears to be rather complex. 'Straggling' increases with ϵ_{max} which in turn increases rapidly with p_0 (roughly quadratically in the few-GeV region [8]) thus favoring lower muon energies. However, one must clearly stay well above $p_0 \approx 0.3$ GeV/c where dE/dx is minimum. Also at these lower momenta thinner cooling targets are indicated and muon decay becomes more probable. The information in figs. 2–5 is also relevant in this regard. The above complications do not necessarily detract from the merits of ionization cooling but it appears that care must be taken in optimizing the available parameters to achieve worthwhile reductions in phase space.

Acknowledgement. My thanks to R. Noble for helpful discussions and to C. Ankenbrandt and N. Mokhov for comments on the manuscript.

References

[1] A. N. Skrinsky, Proc. 20th Int. Conf. on High Energy Physics, A.I.P. Conf. Proc. 68 (1980) 1056.

[2] D. Neuffer, Particle Accelerators 14 (1983) 76.

[3] L. Landau, J. Phys. (USSR) 8 (1944) 201.

[4] P. V. Vavilov, J. Exptl. Theoret. Phys. (USSR) 32 (1957) 920; transl. Sov. Phys. JETP 5 (1957) 749.

[5] S. M. Seltzer and M. J. Berger, in *Studies in Penetration of Charged Particles in Matter*, Publ. 1133, Nat. Acad. Sci–Nat. Res. Council, Washington, DC (1964).

[6] Energy transfers of the order of the electron binding energy and below do not follow the ϵ^{-2} law. However the larger energy losses will dominate the fluctuations in overall loss and a crude treatment of the smaller losses is sufficient, see [3] and also R. Talman, Nucl. Inst. Meth. 159 (1979) 189.

[7] H. J. Bhabha, Proc. Roy. Soc. 164 (1938) 257.

[8] The exact expression of ϵ_{max} is

$$\epsilon_{max} = \frac{2m_e\beta^2\gamma^2}{1 + 2\gamma m_e/m_\mu + (m_e/m_\mu)^2}. \tag{14}$$

In [4] Vavilov exhibits—but makes no explicit use of—a frequently used approximate formula which ignores the last two terms in the denominator. This is justified only for $\gamma \ll m_\mu/m_e$ where $\gamma = (1-\beta^2)^{-1}$. When Vavilov's distributions—for a given β and κ—are presented as in fig. 1 (or as in refs. [4, 5]) ϵ_{max} enters only via the definition of κ and λ.

[9] L. Montanet et al., Phys. Rev. D50 (1994) 1177.

[10] J. D. Jackson, *Classical Electrodynamics*, 2nd Ed., J. Wiley, New York, 1975, pp. 450ff.

[11] B. Rossi, *High-Energy Particles*, Prentice-Hall, Englewood Cliffs, N.J., 1952, pp. 63ff.

[12] M. N. Rosenbluth, Phys. Rev. 79 (1950) 615.

[13] Y. S. Tsai, Rev. Mod. Phys. 46 (1974) 815.

[14] G. Reading Henry, Phys. Rev 151 (1966) 875.

[15] W. Czyz and K. Gottfried, Ann. Phys. (N.Y.) 21 (1963) 47; W. Czyz, Phys. Rev. 131 (1963) 2141.

[16] A. Van Ginneken, Nucl. Inst. Meth. A251 (1986) 21.

[17] The 14 MeV in eq. (17) of [2] applies to a projected *rms* angle [9] which makes the factor of 1/2 in eqs. (18-20) of [2] redundant, which thus understates the equilibrium emittance.

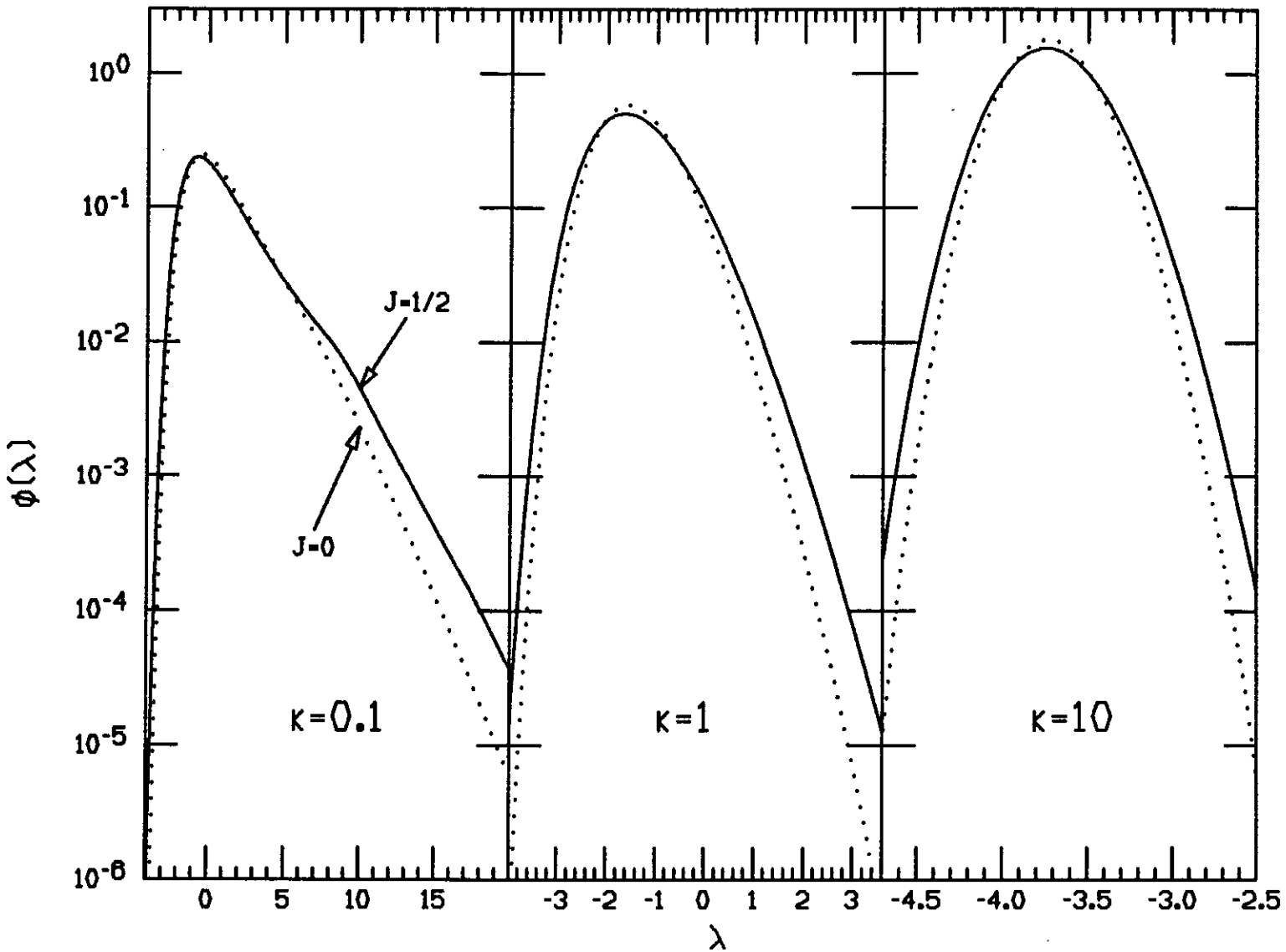

Fig.1 Comparison of Vavilov distributions for J=0 and J=1/2 for β=1 and for different values of κ.

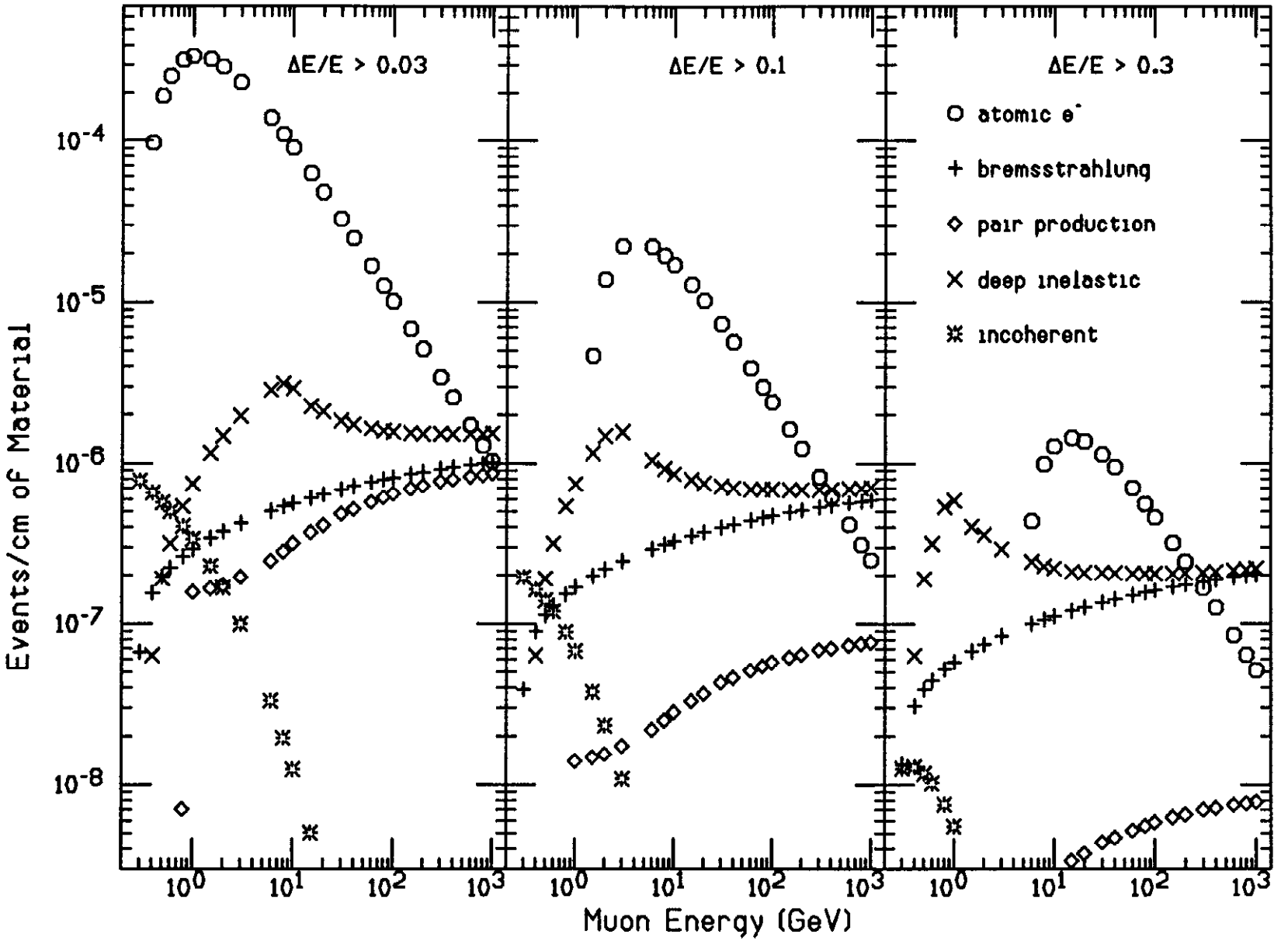

Fig. 2 Number of events per cm with ΔE/E > 0.03, 0.1, and 0.3 in an individual collision for lithium target and for the indicated mechanisms.

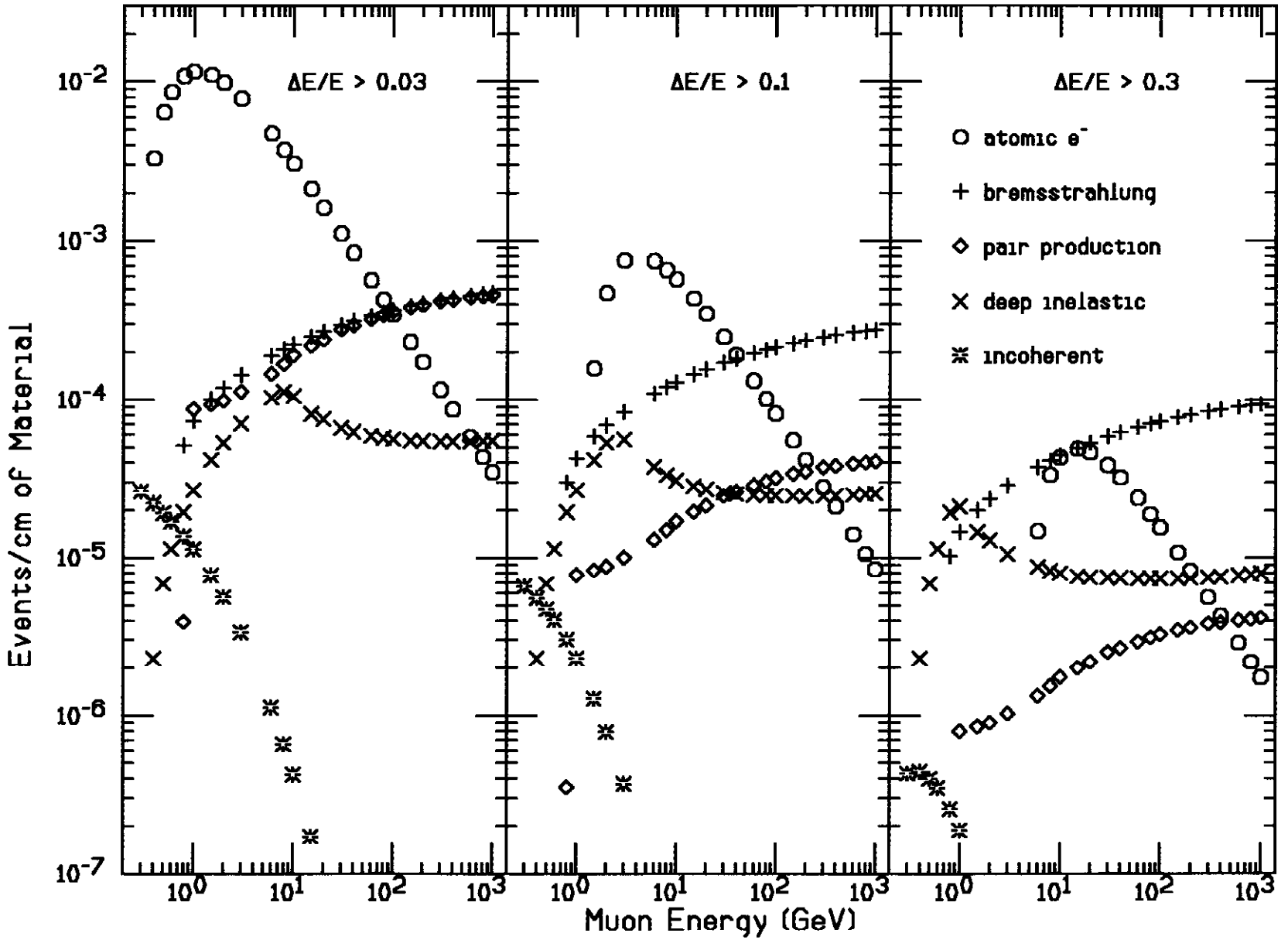

Fig. 3 Number of events per cm with ΔE/E > 0.03, 0.1, and 0.3 in an individual collision for tungsten target and for the indicated mechanisms.

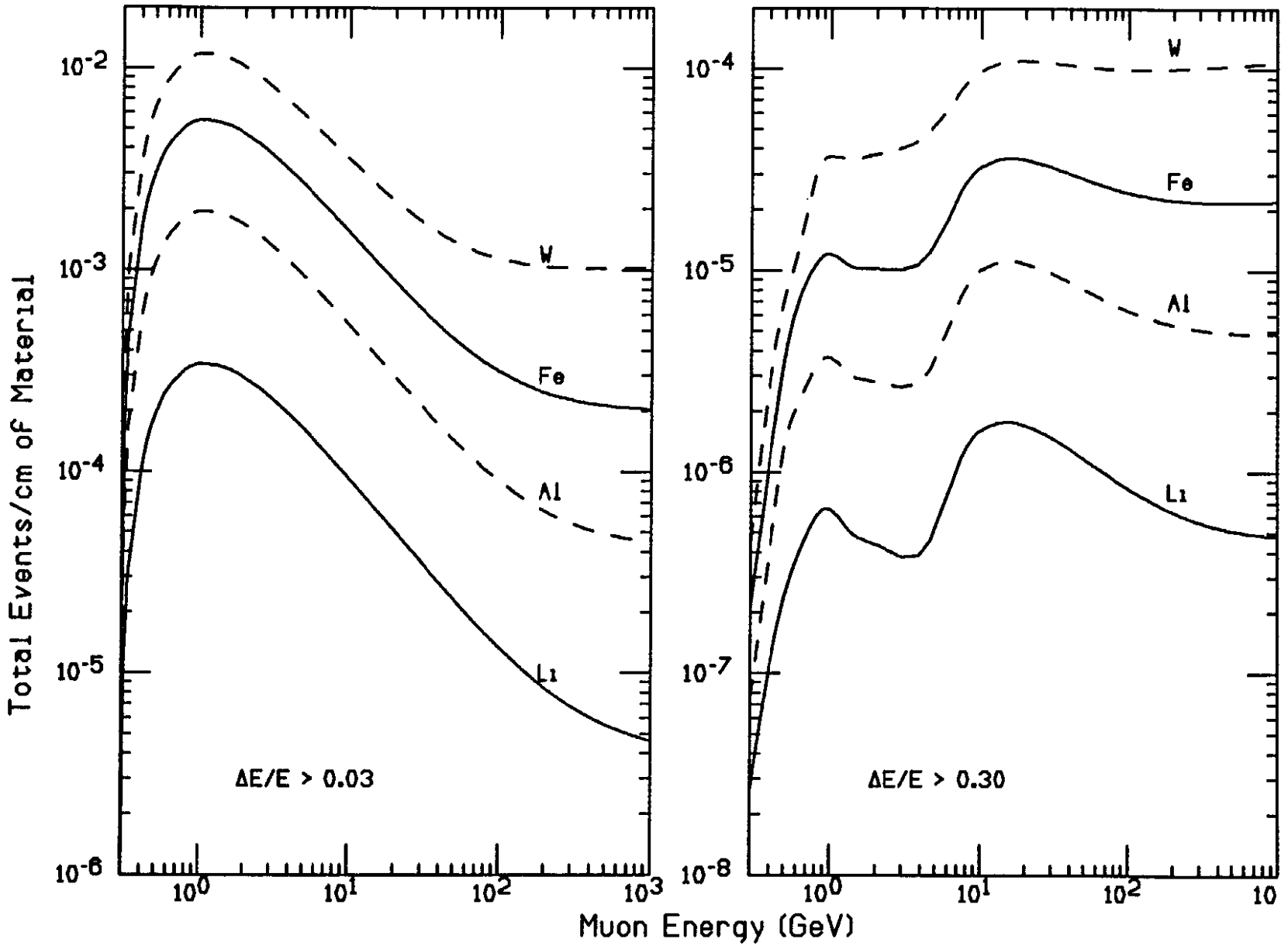

Fig. 4 Total number of events per cm with ΔE/E > 0.03 and 0.3 in an individual collision for various targets.

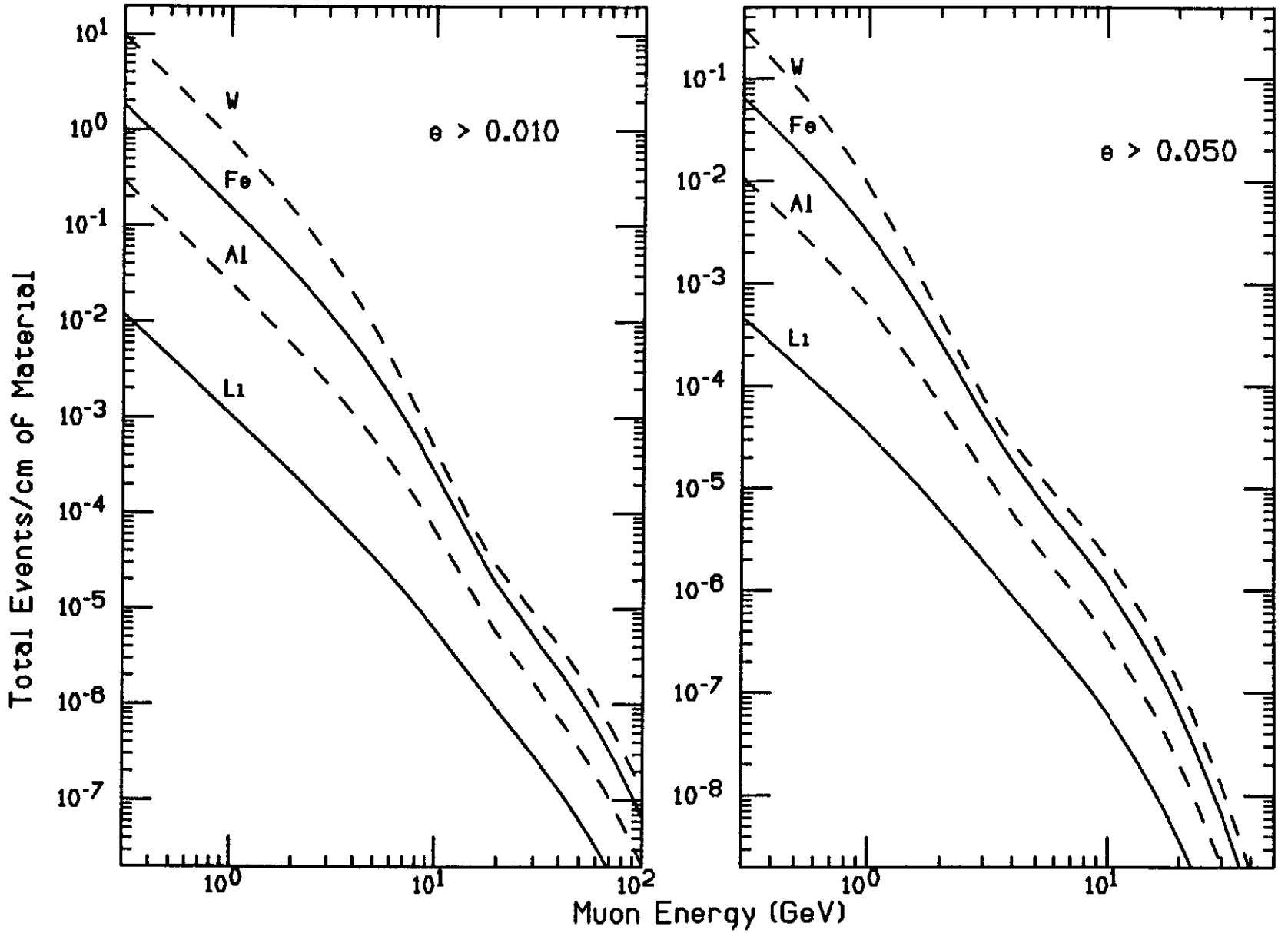

Fig. 5 Total number of events per cm with $\Delta e > 0.01$ and 0.05 in an individual collision for various targets.

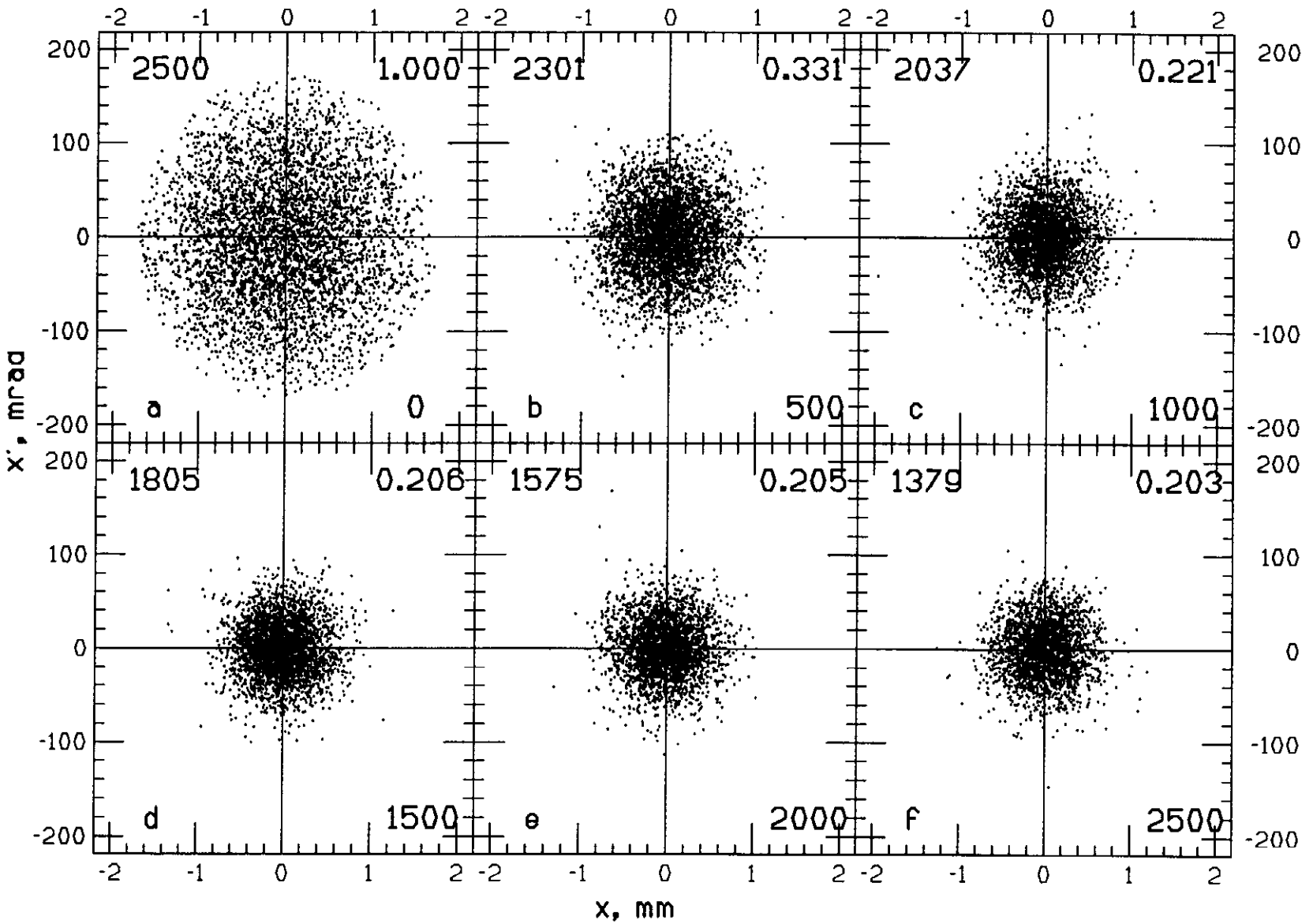

Fig. 6 Evolution of transverse phase space for 1 GeV muons repeatedly traversing 1 cm beryllium target. Indicated in each plot are the remaining number of muons (upper left) and their relative effective phase space area (upper right) for the number of traversals (lower right).

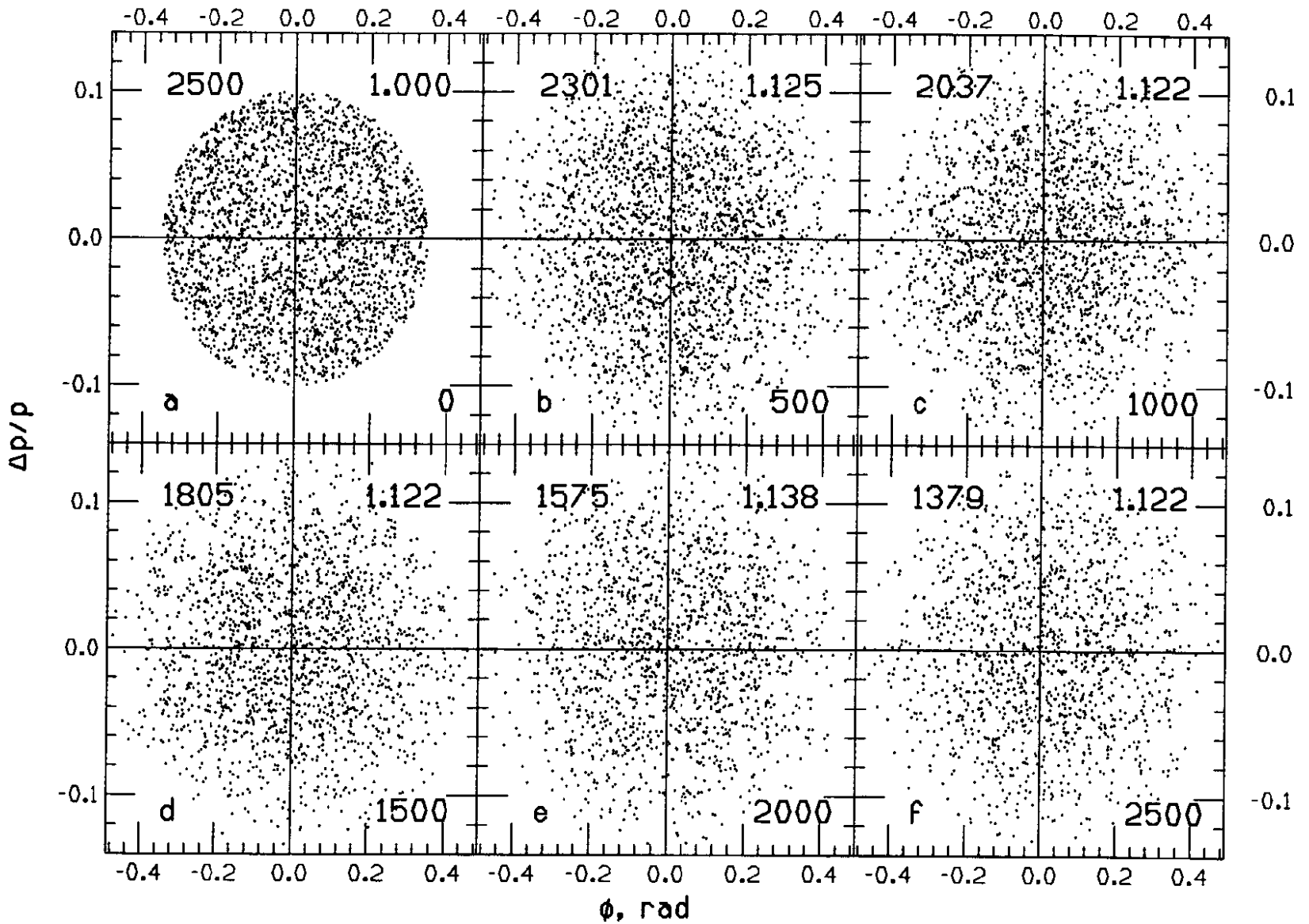

Fig. 7 Evolution of longitudinal phase space for 1 GeV muons repeatedly traversing 1 cm beryllium target. Indicated in each plot are the remaining number of muons (upper left) and their relative effective phase space area (upper right) for the number of traversals (lower right).

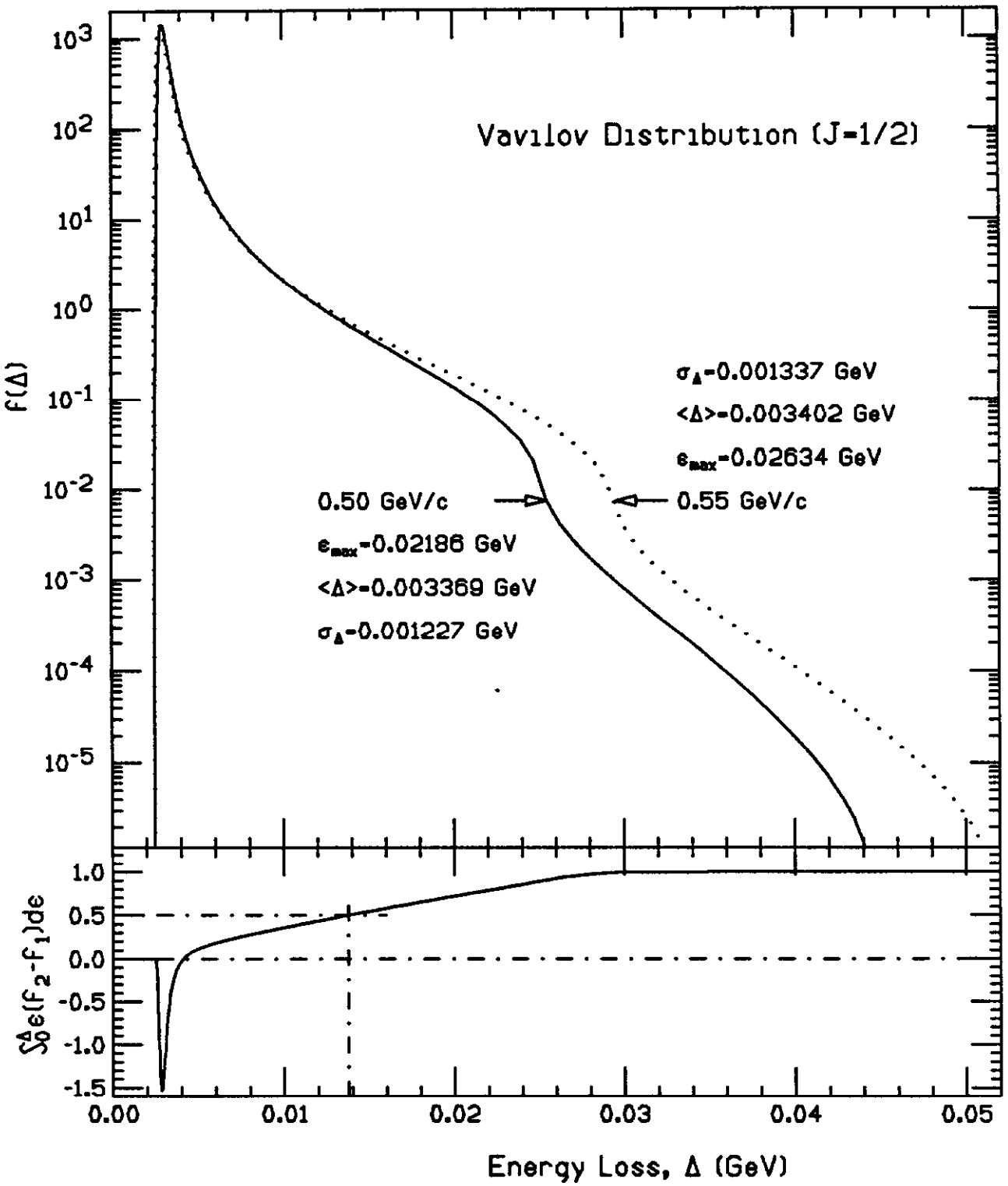

Fig. 8 Upper: Distribution of ionization energy deposited in 1 cm Be target by muons of 0.50 and 0.55 GeV/c. Lower: Integral of energy-weighted difference between 0.55 and 0.5 GeV/c curves normalized to total difference.

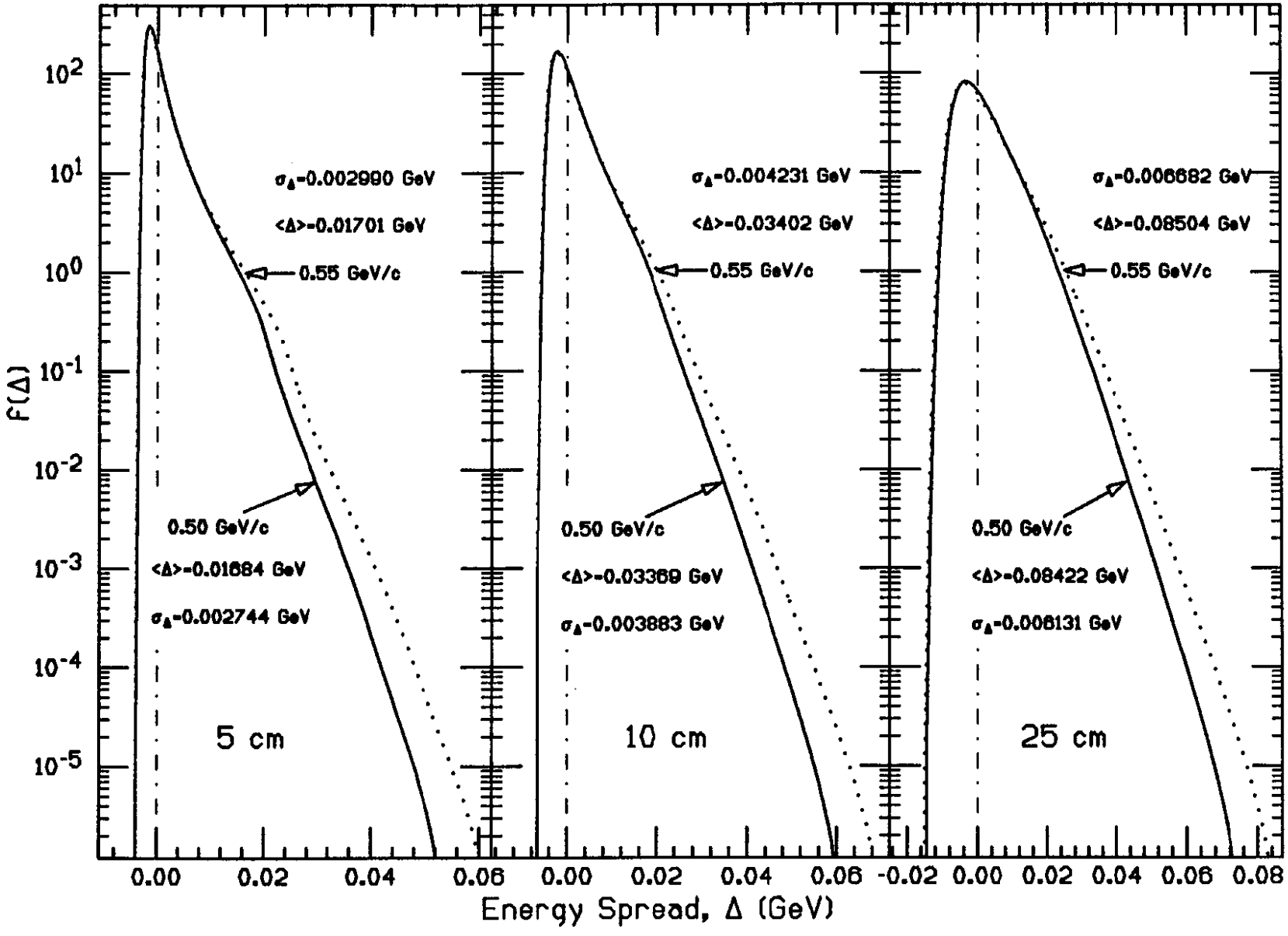

Fig. 9 Energy spread of mono-energetic muons in Be targets by 0.5 and 0.55 GeV/c muons.